Journal of Applied Mechanics and Technical Physics, Vol. 49, No. 6, pp. 891–898, 2008

GAS-DYNAMIC SIGNS OF EXPLOSIVE ERUPTIONS OF VOLCANOES. 1. HYDRODYNAMIC ANALOGS OF THE PRE-EXPLOSION STATE OF VOLCANOES, DYNAMICS OF THE THREE-PHASE MAGMA STATE IN DECOMPRESSION WAVES

V. K. Kedrinskii

UDC 532.593+532.529+532.528+532.787+550.3

Experimental data and results of numerical simulations of the magma state dynamics in explosive eruptions of volcanoes are presented. The pre-explosion state of volcanoes and the cavitation processes developed in the magma under explosive decompression are studied under the assumption that the intensity of explosive volcanoes does not exert any significant effect on the eruption mechanisms. In terms of the structural features of the pre-explosion state, a number of explosive volcanic systems are close to hydrodynamic shock-tube schemes proposed by Glass and Heuckroth. High-velocity processes initiated by shock-wave loading of the liquid may be considered as analogs of natural volcanic processes, which have common gas-dynamic features and common kinetics responsible for their mechanisms, regardless of the eruption intensity.

Key words: *magma state dynamics, explosive eruption, simulations, cavitation, crystallization, destruction.*

Introduction. Explosive volcanic eruptions comprise a wide range of predictable processes, which primarily involve phase transitions induced by decompression of the liquid magma previously compressed to high pressures. As a consequence, the magma solution containing large amounts of dissolved gases becomes oversaturated. Homogeneous nucleation generates cavitation nuclei growing, in particular, by the mechanism of gas diffusion from the melt. The melt viscosity dynamically increases during the degassing process. At the same time, the mechanisms of many processes that occur in the magma and determine the magma state dynamics and the formation of the flow structure in decompression waves, as well as the character of the eruption proper, remain unclear. As the answers to these questions cannot be unambiguous because the phenomena are extremely complicated and involve many aspects and many scales, a classification of volcanic systems was obviously needed.

Apparently, the first classification (in terms of the eruption character) was proposed at the end of the 19th century. In this classification, all known volcanoes were divided into three groups: 1) quiet volcanoes (which produce flowing lava); 2) explosive volcanoes; 3) intermediate volcanoes (violent eruptions followed by lava flows). A physical model was formulated for the initial state of explosive volcanoes, where the magma becomes sufficiently cooled to produce a lava plug blocking the gases and the magma in the volcanic conduit. When the pressure in the conduit reaches a value sufficient to destroy the plug, the hot gases and the magma explode out of the volcano.

In 1908, Lacroix refined the notion of explosive volcanoes on the basis of the eruption intensity. In his classification, explosive volcanoes are divided into the following groups (of increasing intensity): Hawaiian (eruptions that rarely have an explosive character), Strombolian (moderate eruptions), Plinian/Vulcanian (strong eruptions), and Pelean (greatest eruptions) volcanoes. A question arises: Are these processes with many aspects governed by identical mechanisms? Obviously, the answer to this question will provide better understanding of the processes inside the magma and allow simulating the magma state dynamics during explosive decompression.

Lavrent'ev Institute of Hydrodynamics, Siberian Division, Russian Academy of Sciences, Novosibirsk 630090; kedr@hydro.nsc.ru. Translated from Prikladnaya Mekhanika i Tekhnicheskaya Fizika, Vol. 49, No. 6, pp. 3–12, November–December, 2008. Original article submitted January 28, 2008.

An analogy for the processes inherent in explosive volcano eruptions can be found in hydrodynamics of high-velocity liquid flows initiated by explosive sources of different intensity. The latter depends on the energy release rate, which is insignificant in the case of underwater explosions of wires or gaseous mixtures and reaches a maximum value in the case of explosions of condensed cast and pressed explosives. As an example, we can mention a directed jet flux (fountain) on the free surface of a liquid, which is observed in shallow underwater explosions and resembles volcanic eruptions [1]. It should be noted that the mechanics of these phenomena has the same cumulative nature determined only by the interaction of the explosive cavity with the free surface and independent of the energy release rate of the explosive sources.

For some volcanoes included into Lacroix's classification, the intensity may also be assumed to exert no significant effect on the mechanisms responsible for the processes inherent in eruptions. An important milestone is the search for common features of explosive eruptions to form physical grounds for mathematical models and experimental approaches. A possibility of classifying the processes of formation of high-velocity flows in conduits in terms of common gas-dynamic signs and common kinetics determining the structure of these flows is studied in the paper.

Some gas-dynamic features of explosive eruptions are considered below.

1. Hydrodynamic Shock Tubes as Analogs of the Scheme of the Pre-Explosion State of Volcanoes. An analysis of research in the field of mechanics of liquid destruction under shock-wave loading [2] and data on volcanic eruptions presented, in particular, in [3] allows two basic conclusions to be drawn. First, at least some volcanoes classified geophysically as explosive volcanoes are similar to hydrodynamic shock tubes (GDSTs) in terms of their structure and pre-eruption features. Second, unsteady high-velocity processes initiated by pulsed loading of liquid media [2] can be considered under certain conditions as analogs of natural volcanic processes in terms of both the probable mechanisms of their initiation and the flow state dynamics.

Various types of hydrodynamic shock tubes designed for generation of shock waves with controlled parameters under laboratory conditions may be used in experimental modeling of explosive eruptions [4–6]. For modeling the processes developed in the compressed magma subjected to decompression, it suffices to change the places of the gas and the liquid sample in the static scheme proposed by Glass and Heuckroth [4]. Dynamic schemes [5, 6] that allow generation of shock waves with given parameters involve only liquid samples with the free surface and do not operate with notions of the high-pressure chamber and diaphragm in the sense of the static scheme [4]. In this case, the gas-dynamic scheme of the pre-explosion state of the volcano is formed in the dynamic mode. The sample, which has an interface with the atmosphere (free surface), is compressed to a given pressure by a shock wave generated by some external source [5, 6] and propagating over the sample up to the interface, thus, simulating the hydrostatic situation in the volcanic chamber. The wave reflected from the interface is a rarefaction wave, which propagates over the compressed sample in the opposite direction and acts as a decompression wave.

Obviously, the layout of the shock tube [4] (Fig. 1a) is a close analog of the hydrodynamic scheme of volcanoes with channels (conduits) closed by the solidified lava: the so-called domes if they are located on the bottom of the crater or plugs if they are formed in the channel proper. Indeed, the HDST scheme [4] includes three basic elements: a high-pressure chamber p_+ (analog of the system consisting of a volcanic chamber and a channel filled by the magma), a low-pressure chamber p_- (analog of the free portion of the volcanic conduit or a crater contacting the atmosphere), and a diaphragm (plug) d separating these two chambers (Fig. 1a). The diaphragm coordinate is $x = 0$. Breakdown of the diaphragm d converts the system to a state called the discontinuity decay in gas dynamics; as a result, a rarefaction (decompression) wave emerges in the high-pressure chamber and propagates over the system. This is the initial stage of the eruption, which actually creates the structure of the magma flow and conditions for its transition to a two-phase state. Phase transitions and dynamically developing bubble cavitation in liquid media are known to change substantially the parameters and structure of the pulsed field of tensile stresses initiating these processes [2]. Similar effects can be naturally expected in volcanic systems as well.

Some specific features of the wave field dynamics in a medium with developing cavitation can be qualitatively demonstrated by a simple example: the high-pressure chamber (the scheme proposed in [4] is considered) is occupied by a water sample compressed to a pressure $p_+ = 1.5$ atm and containing heterogeneous nuclei of cavitation (microscopic bubbles of the free gas with a radius $R_0 = 50$ μm and a volume fraction of the gas $k_0 = 10^{-4}$). The process of formation of the wave field structure in such a medium after diaphragm breakdown was calculated in [7] (Figs. 1b–1d) within the framework of the two-phase Iordansky–Kogarko–van Wijngaarden model [8–10].

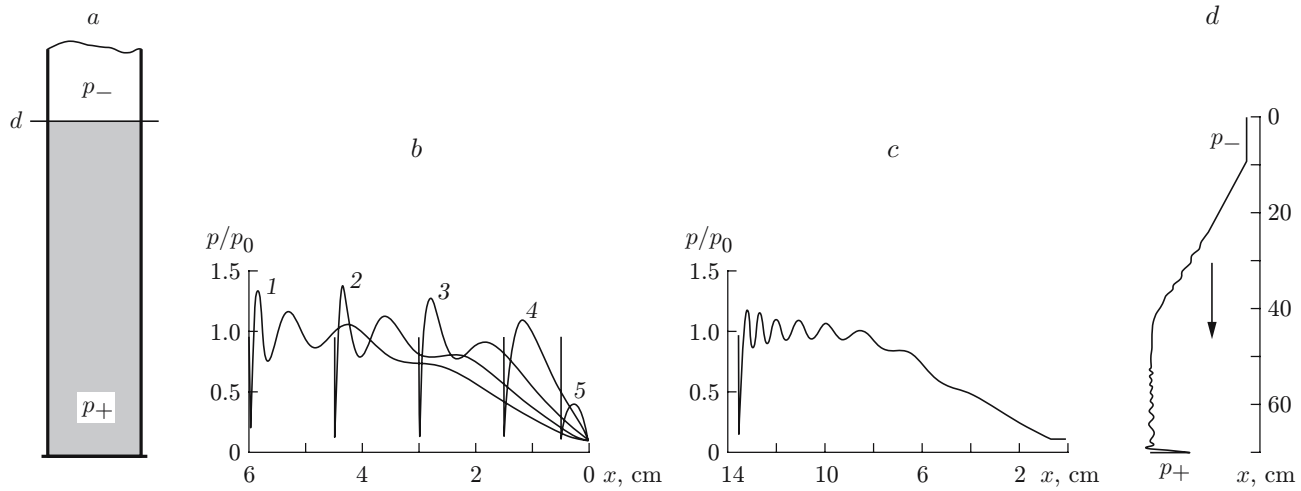

Fig. 1. Calculated wave structure in a cavitating medium ($x > 0$) in the high-pressure chamber: (a) shock tube layout [4]; (b) formation of a precursor [t = 3.3 (1), 10 (2), 20 (3), 30 (4), and 40 μsec (5)]; (c) distribution of pressure p/p_0 at $t = 90$ μsec; (d) profile of the rarefaction wave at $t = 440$ μsec (the arrow indicates the direction of the wave front motion).

It follows from Fig. 1b that a centered rarefaction wave is generated in the unloaded pre-compressed medium during the initial period after the discontinuity decay. This rarefaction wave propagates over the undisturbed medium to the left with a "frozen" velocity of sound $c_0 = 1.5 \cdot 10^3$ m/sec and initiates the cavitation process. The wave profile is transformed to a wave packet [7]. It follows from Figs. 1c and 1d, which show the wave field structure at $t = 90$ and 440 μsec, that the structure includes a precursor (wave packet) and the main rarefaction wave with an oscillating front. The wave front (Fig. 1d) propagates with an equilibrium phase velocity of sound $c_{ph} = \sqrt{\gamma p_0/(\rho_0 k_0)}$ typical of a two-phase bubble medium (in the case considered, approximately 10^3 m/sec).

Obviously, the most clear example of explosive volcanoes with the pre-explosion state corresponding to the scheme proposed in [4] is the St. Helen volcano whose powerful eruption was initiated by a huge landslide, which tore off the plug closing the volcano vent, as geophysicists believe. In accordance with this scheme, the pre-eruption state of the volcano (Fig. 2a) can be reconstructed from its post-eruption state described in [11].

The same scheme is observed in some open volcanic systems due to natural processes that occur during deformation of a crater containing liquid lava (for instance, the Kilauea volcano on the Hawaiian Islands). As was reported by American geophysicists, crater sloughing and underground water in the vicinity of the volcanic vent initially protected by a ground shell played an important role in the 1924 explosive eruption of the Kilauea volcano (Fig. 2b). According to this interpretation, the melted lava was responsible for sloughing of the crater walls and some part of the protective shell of the vent. The sloughed rocks formed a magma-blocking plug in the volcanic vent mouth, thus, forming the initial state of the system corresponding to the scheme proposed in [4].

The high pressure of the vapor formed owing to interaction of seeping underground water with the lava, broke the plug and led to an explosive eruption. Note that the mechanism of initiation of the Kilauea volcano eruption, remaining intact as a whole, could have had a somewhat different character if the plug formed after sloughing were assumed to be permeable both for the underground water and for the magma. It could be naturally expected that the vapor produced by their interaction filled the plug pores, thus, converting the latter into something like a vapor "bomb," which could initiate the eruption when the vapor pressure reached high values.

Figure 2b shows the initial shape of the Kilauea volcano crater (before its walls were destroyed by the hot lava) and the final shape (after destruction of the walls and plug formation). It is seen that the hydrodynamic schemes of the St. Helen volcano (Fig. 2a) and the Kilauea volcano (scheme II in Fig. 2b) are actually physical analogs of the classical scheme [4] (see Fig. 1a). Thus, this scheme can be used both to arrange experiments and to perform mathematical simulations of the magma behavior in the decompression wave for volcanoes of this type.

The behavior of open volcanic systems was described in [12]. According to these data [12], decompression of the magma uprising from the crust magma chamber toward the Earth's surface leads to gas release (with formation

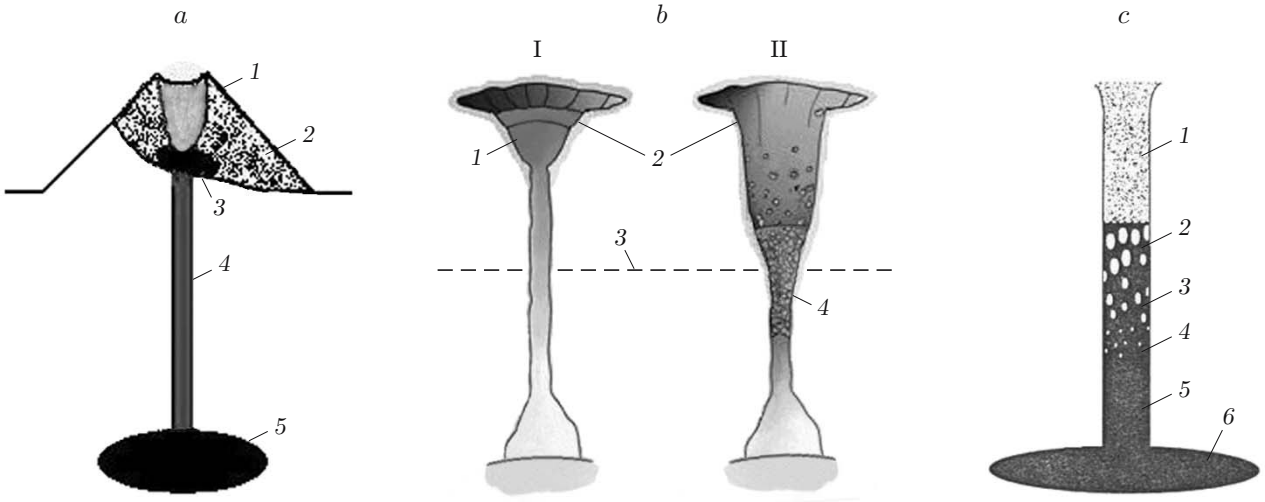

Fig. 2. Schemes of the states of two volcanoes: (a) pre-eruption state of the St. Helen volcano; 1) cone; 2) landslide zone; 3) plug; 4) volcano conduit; 5) volcano chamber; (b) pre-eruption state of the Kilauea volcano; states I and II illustrate the initial shape of the crater and formation of a plug blocking the magma in the channel, resulting from sloughing of the crater walls; 1) lava melt; 2) crater; 3) underground water level; 4) plug; (c) schematic dynamics of the magma flow structure in an open volcanic system [13]; 1) gas and particles; 2) fragmentation zone; 3) foam; 4) cavitation zone; 5) nucleation zone; 6) volcano chamber.

of vapor–gas bubbles); the resultant two-phase mixture becomes swelled, its motion becomes accelerated, and the mixture acquires a foam-like state. Liquid viscous magma films surrounding bubbles in this foam cannot withstand the growing (owing to diffusion from the melt) gas pressure in the bubbles for a long time. The films are destroyed to small fragments and cool down, forming a mixture of ashes and vapor, which moves toward the exit from the conduit to the crater and acquires a high velocity due to free decompression in the atmosphere. Note, if the mixture unloading occurs in the crater proper, the eruption may be much less intense.

Figure 2c shows the scheme of the magma state dynamics [13] corresponding to that described in [12]. It should be noted that this model of the transition from the cavitating state to the foam-like state of the compressed medium owing to explosive unloading agrees with experimental data obtained in accordance with the dynamic HDST scheme [2, 5, 14] in studying problems of cavitating disintegration of liquid media subjected to pulsed loading. Despite the identity of these processes, however, simulations (and primarily experimental modeling) of the magma state dynamics in "stationary-open" volcanic systems that differ from systems of the above-considered type involve certain difficulties. The problem is that the process of decompression initiation by the scheme [12] occurs with a variable mass velocity of magma rising to the Earth's surface rather than with the velocity of sound in the bubbly medium where the decompression wave propagates after the discontinuity decay. Apparently, the mathematical model can capture this feature if the flow velocity and acceleration are determined from the general reasoning. In this case, one can use the formulation of the mathematical problem in accordance with the HDST scheme [4] by imposing a variable decompression wave velocity corresponding to the velocity of upward motion of the magma.

The facts described above actually determine the common gas-dynamic features of the initial state and initial (wave) stage of eruptions of volcanoes of the above-mentioned types: gas-dynamic shock tube scheme, discontinuity decay, and formation of a precursor and a rarefaction (decompression) wave. It should be noted that the wave stage initiated phase transitions, is accompanied by the development of cavitation processes and crystallization, and actually has two characteristic time intervals L_0/c_0 and $L(t)/c_{ph}(k)$ [L_0 is the initial height of the magma column in the volcanic conduit and $L(t)$ is the magma column height changing due to cavitation development]. The first interval is determined by the precursor velocity (velocity of sound c_0 in an undisturbed single-phase medium), and the second interval is determined by the velocity $c_{ph}(k)$ of the main decompression wave in the bubbly medium, which depends on the intensity of cavitation development behind the precursor front and is actually a variable quantity.

2. Gas-Dynamic Model of Bubble Cavitation in the Magma. Role of Crystallites. The presence of crystallites in the magma is an undoubted fact. Their effect on the magma state and on the dynamic processes proceeding in the magma during its decompression, however, are not that clear. Apparently, three states of crystallites can be identified: 1) the crystallite phase is retained, and the crystallites grow in the magma melt, where a third (gaseous) phase (in the form of cavitation bubbles) appears due to homogeneous nucleation in the decompression wave; 2) the crystallites may act as germs for a new (vapor) phase; in this case, the magma melt becomes a two-phase bubbly medium with homogeneous and heterogeneous nucleation proceeding simultaneously or consecutively; 3) in the period between eruptions, the crystallites may form clusters in the volcano channel and in the magma chamber; these clusters can be considered as magma "bombs." Naturally, cavitation nuclei may form both inside the clusters and in the ambient melt.

Let us consider the first variant, where the crystallites initially present in the magma melt act as crystallization germs, and homogeneous nucleation results in intense development of the cavitation process in the zone of action of the decompression wave. The time of cavity nucleation in the magma melt behind the decompression wave front can be determined as the period of induction τ during which the melt in the vicinity of the decompression wave front becomes completely saturated by the nuclei and the magma acquires a three-phase state. The degree of supersaturation of the magma melt remains almost unchanged, and the induction period is determined from the kinetic equations

$$J = J^* \exp\left(-W^*/(k_{\rm B}T)\right), \quad J^* = (2n_g^2 V_g D/d)\sqrt{\sigma/(k_{\rm B}T)}\,, \quad W^* = 16\pi\sigma^3/(3\Delta p^2); \tag{1}$$

$$\Delta p = p_s - p, \qquad V_d = (4\pi/3)(\chi^3 - 1)R^3, \qquad \chi = r_d/R; \tag{2}$$

$$X_d = 1 - \exp\Big(-\int\limits_0^\tau J(t')V_d(t-t')\,dt'\Big), \qquad N_b = \int\limits_0^\tau J(t')(1 - X_d(t'))\,dt'. \tag{3}$$

Here J is the nucleation frequency, n_g is the number of molecules of water dissolved in a unit volume of the magma, V_g is the molecule volume, d is the distance between the molecules, D is the diffusion coefficient of the gas in the melt, σ is the surface tension, W^* is the work spent on formation of critical nuclei, r_d is the radius of the nuclei with the diffusion layer, R is the radius of the nuclei, V_d is the volume of the diffusion layer, X_d is the total volume of diffusion layers in a unit volume of the magma, N_b is the density of cavitation nuclei in a unit volume of the magma, and $k_{\rm B}$ is the Boltzmann constant. The calculations were performed for the following initial data: height of the magma column in the volcano conduit 1 km (with the corresponding distribution of hydrostatic pressure in the gravity field), pressure in the volcanic chamber $p_{\rm ch} = 170$ MPa, temperature of the melt $T = 1120$ K, density of the melt 2650 kg/m^3, and distribution of viscosity over the column height in the interval 10 Pa $\cdot$ sec $< \mu < 10^3$ Pa $\cdot$ sec.

The calculations showed that decompression on the rarefaction wave front initiating the nucleation process is formed after discontinuity decay (formation of the free surface of the magma column) only by the time $t \approx 14$ msec. The value of J is of the order of unity. The value of N_b is approximately 0.1 m^{-3}. These characteristics dynamically increase within several milliseconds: $J \approx 10^5$ and $N_b > 10$ m^{-3} for $t = 15$ msec and $J \approx 10^9$ and $N_b \approx 10^5$ m^{-3} for $t = 16$ msec; for $t = 17$ msec, the maximum values of both the nucleation frequency and the density of cavitation nuclei are reached: $J \approx 10^{14}$ and $N_b \approx 10^9$ m^{-3}. Thus, the time $t = 17$ msec can be considered as the instant when the melt becomes saturated by nuclei. It should be noted that the bubble radii, the viscosity and its distribution, and the concentration of the gas phase in the melt before this instant remain almost unchanged. After saturation, the radius of the cavitation bubbles behind the decompression wave front increases to 25 μm within several hundreds of microseconds. Later on, however, the bubble growth becomes slower. For example, the bubble radii reach 65 μm at $t = 41$ msec.

According to the data cited above, when the decompression capable of initiating the phase transition is reached, the induction period of the three-phase state is approximately 2 msec (from the time $t = 15$ msec till $t = 17$ msec), which are necessary for the melt to become saturated by nuclei. After that moment, the decompression front can be considered both as the front of saturation of the melt by nuclei and as the diffusion front, because the gas diffuses from the melt in what follows to already available cavitation nuclei, and practically no new nuclei are formed.

The next stage of the dynamics of the volcano state can be determined as the stage of development of the cavitation process in the magma melt. The duration of this stage is longer by several orders of magnitude, and it is this stage that determines the flow structure in the volcanic conduit. Apparently, it was first demonstrated in [15] that both the cavitation development process and the dynamics of the wave field structure in the cavitation zone can be described by a system of equations of unsteady gas dynamics [8–10] with the mean values of pressure, density, and mass velocity. The system is supplemented by kinetic relations including the Rayleigh equation, where the pressure at infinity is replaced by the mean pressure in the medium. This model was demonstrated to provide an adequate description of experimental data [2, 15, 16].

For simulating the process of cavitation development in the magma melt, we use the HDST scheme [4] and the gas-dynamic model [8–10, 15] with the Navier–Stokes equation written in the general case for the viscosity variable instead of the Euler equation. The conservation laws are commonly known; hence, we give only the system of closing kinetic equations, including the Rayleigh equation, which determine the dynamics of the state of the two-phase medium under consideration:

$$p = p_0 + \frac{\rho_{l0} c_{l0}^2}{n}\Big[\Big(\frac{\rho}{\rho_{l0}(1-k)}\Big)^n - 1\Big], \qquad \frac{4\pi}{3}\, p_g R^3 = \frac{m_g k_{\rm B} T}{M}; \tag{4}$$

$$R\ddot{R} + \frac{3}{2}\,\dot{R}^2 = \frac{p_g(R) - p}{\rho_{l0}} - \frac{4\mu\dot{R}}{\rho R}, \quad \mu = \mu^* \exp\Big(\frac{E_\mu(C)}{k_{\rm B} T}\Big), \quad E_\mu(C) = E_\mu^*(1 - k_\mu C); \tag{5}$$

$$\frac{dm_g}{dt} = 4\pi R^2 \rho D\Big(\frac{\partial C}{\partial r}\Big)_R = 4\pi R \rho D(C_i - C^{eq}(p_g)). \tag{6}$$

Equations (4) describe the states of the bubbly medium $p(\rho)$ and the gas, and Eqs. (5) determine the cavitation bubble radii $R(p, p_g, \mu)$ and the viscosity $\mu(C)$ [17], which depends on the dynamics of the concentration C of gases dissolved in the magma. Equation (6) is the diffusion equation. Kedrinskii et al. [18] supplemented the system of kinetic equations by equations of crystallization, including the equation of temperature balance in the three-phase magma and equations for determining the crystallization velocity $v_{\rm cr}$ and the specific volume of the crystallized magma $k_{\rm cr}$:

$$\frac{dT}{dt} = {\rm Ku}\,\frac{dX}{dt} - {\rm Ku}'\,\frac{4\pi}{3}\,N_b z_0^3\,\frac{dm_g}{dt},$$

$$k_{\rm cr} = \frac{4\pi}{3}\,N_{\rm cr} v_{\rm cr0}^3 t_0^3\Big(\int\limits_0^t v_{\rm cr}\,d\tau\Big)^3, \quad v_{\rm cr} = \Delta T. \tag{7}$$

Here Ku and Ku′ are Kutateladze crystallization and desorption numbers, respectively; the quantities marked by the zero subscript are the scales used for normalization of variables.

The mathematical model with kinetics (1)–(7) [18] allowed a pioneering analysis of the dynamics of the state of the heavy magma in the volcano conduit in a nonstationary wave field and the basic characteristics of this field. As was shown in [18], the distribution of the volume concentration of the bubbles k_b is already formed by the time $t \approx 4$ sec and changes little in what follows (Fig. 3). This means that the bubble growth in the melt becomes much less intense, and the bubble size (with allowance for an increase in the magma viscosity by 6 to 7 orders) approaches the maximum possible value (Fig. 4). The calculations (see Figs. 3 and 4) allow us to assume that the glass transition on the major part of the magma column is almost completed by the time $t \approx 6$ sec after the beginning of unloading in the three-phase magma with "frozen" bubbles having radii of approximately 0.3 mm.

However strange it may seem, but a drastic increase in magma viscosity during degassing and diffusion process that finally determines the dynamics of growth of cavitation bubbles can substantially simplify mathematical modeling of the process, if it turns out that the Rayleigh equation is valid at the initial stage only. In this case, the growth of bubbles at a certain stage is predominantly determined by the diffusion process; the Rayleigh equation becomes "blocked" and can be replaced by the analytical dependence $R(t)$ [17] in the system of kinetic equations.

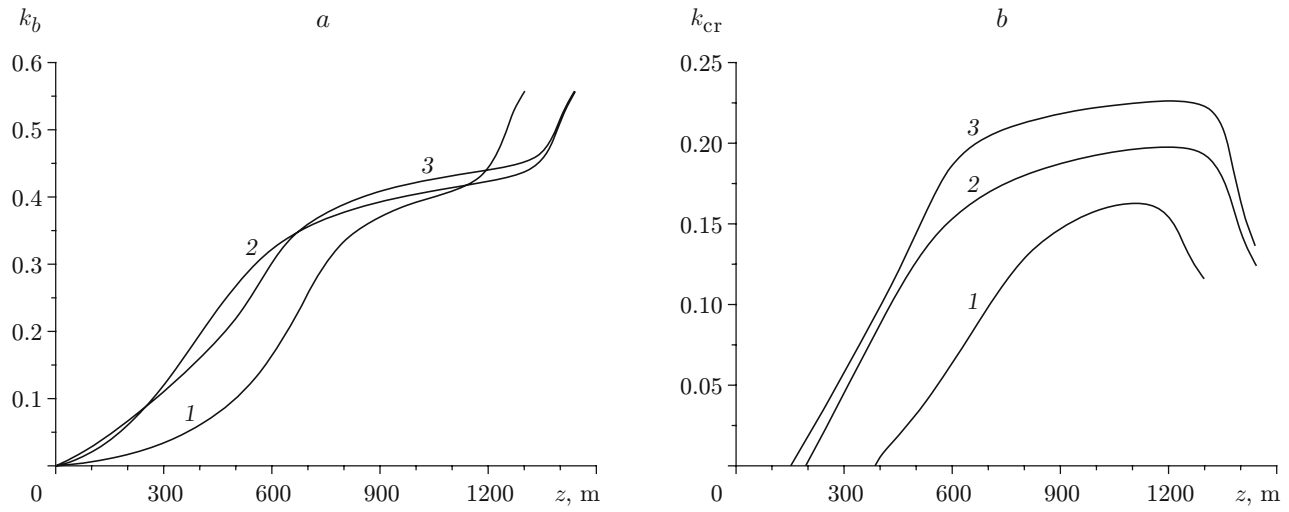

Fig. 3. Dynamics of the distribution of the concentrations of the gaseous phase (a) and crystalline phase (b) over the z coordinate at different times after diaphragm breakdown: $t = 2.1$ (1), 3.8 (2), and 6.1 sec (3).

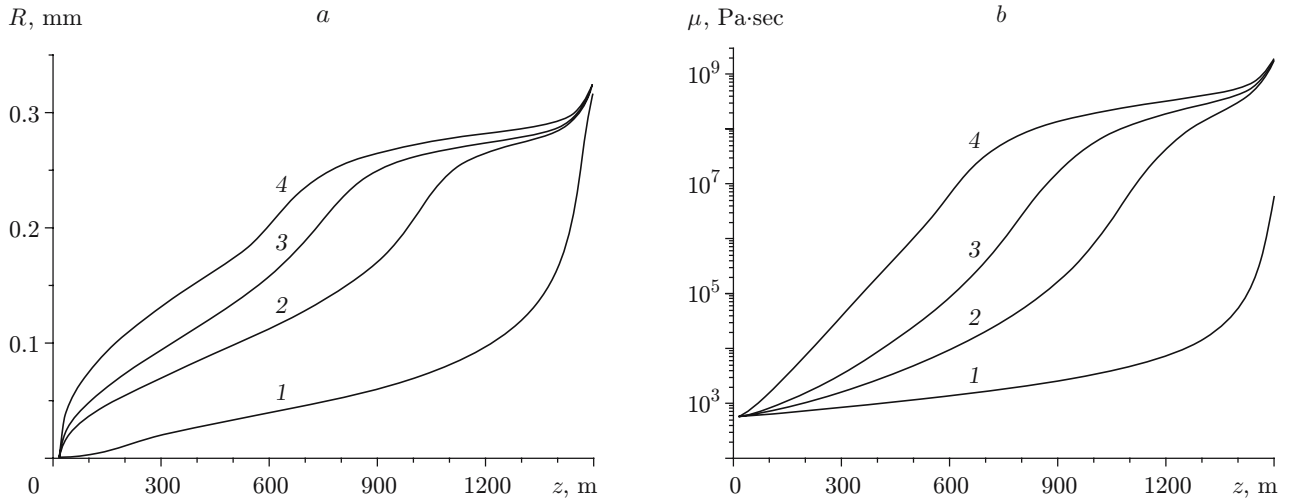

Fig. 4. Dynamics of the distribution of the bubble radius (a) and viscosity (b) over the z coordinate at different times after diaphragm breakdown: $t = 0.6$ (1), 2.1 (2), 3 (3), and 5.8 sec (4).

Conclusions. The analysis of the pre-explosion state of volcanoes included into Lacroix's classification in terms of eruption intensity shows that the structural features of these volcanic systems are almost identical and close to hydrodynamic shock tubes corresponding to schemes proposed by Glass and Heuckroth. The proposed mathematical model of multiphase media and the numerical analysis performed allow us to assume that phase transitions in the compressed heavy magma and the dynamics of the magma state under sudden decompression (at least, before the destruction stage) can be described by a system of gas-dynamic conservation laws with a wide range of kinetic relations taking into account the characteristic features of physical processes in the magma.

This work was supported by the Russian Foundation for Basic Research (Grant No. 06-01-00317a) and by the Integration Project No. 4.14.4 of the Siberian Division of the Russian Academy of Sciences.

REFERENCES

1. V. K. Kedrinskii, "The experimental research and hydrodynamic models of a "sultan," *Arch. Mech.*, **26**, Nos. 3/4, 535–540 (1974).
2. V. K. Kedrinskii, "Nonlinear problems of cavitation breakdown of liquids under explosive loading (review)," *J. Appl. Mech. Tech. Phys.*, **34**, No. 3, 361–377 (1993).
3. J. S. Gilbert and R. S. J. Sparks (eds.), *The Physics of Explosive Volcanic Eruptions* (Geological Society Special Publication), Vol. 145, Geolog. Soc., London (1998).
4. I. I. Glass and L. E. Heuckroth, "Hydrodynamic shock tube," *Phys. Fluids*, **6**, No. 4, 543–549 (1963).
5. M. I. Vorotnikova, V. K. Kedrinskii, and R. I. Soloukhin, "Shock tube for investigating one-dimensional waves in liquids," *Combust., Expl., Shock Waves*, **1**, No. 1, 3–9 (1965).
6. A. S. Besov, V. K. Kedrinskii, and E. I. Pal'chikov, "Studying of the initial stage of cavitation using the diffraction-optical method," *Pis'ma Zh. Tekh. Fiz.*, **10**, No. 4, 240–244 (1984).
7. V. K. Kedrinskii and S. I. Plaksin, "Rarefaction wave structure in cavitating liquid," in: *Proc. of the 11th Int. Symp. on Nonlinear Acoustics* (Novosibirsk, August 24–28, 1987), Vol. 1, Sib. Branch USSR Acad. Sci., Novosibirsk (1987), pp. 51–55.
8. S. V. Iordanskii, "Equations of motion of a liquid containing gas bubbles," *Prikl. Mekh. Tekh. Fiz.*, No. 3, 102–110 (1960).
9. B. S. Kogarko, "One model of a cavitating liquid," *Dokl. Akad. Nauk SSSR*, **137**, No. 6, 1331–1333 (1961).
10. L. Van Wijngaarden, "On the equations of motion for mixtures of liquid and gas bubbles," *J. Fluid Mech.*, **33**, 465–474 (1968).
11. J. Eichelberger, E. Gordeev, and T. Koyaguchi, "A Russian–Japan–US partnership to understand explosive volcanism," http://www.uaf.edu/geology/PIRE/PIRE.pdf, Jun. 22 (2006), pp. 1–4.
12. A. W. Woods, "The dynamics of explosive volcanic eruptions," *Rev. Geophys.*, **33**, No. 4, 495–530 (1995).
13. F. Dobran, "Non-equilibrium flow in volcanic conduits and application of the eruption of Mt. St. Helens on May 18 1980 and Vesuvius in Ad. 79," *J. Volcanol. Geotherm. Res.*, **49**, 285–311 (1992).
14. A. R. Berngardt, E. I. Bichenkov, V. K. Kedrinskii, and E. I. Pal'chikov, "Optic and x-ray investigation of water fracture in rarefaction wave at later stage," in: *Proc. of the IUTAM Symp. on Optical Methods in the Dynamics of Fluids and Solids* (Prague, September 17–21, 1984), Springer, Berlin (1985), pp. 137–142.
15. V. K. Kedrinskii, "Dynamics of the cavitation zone during an underwater explosion near a free surface," *J. Appl. Mech. Tech. Phys.*, **16**, No. 5, 724–733 (1975).
16. V. K. Kedrinskii, "Shock induced cavitation," in: *Shock Wave Sciences and Technology Reference Library*, Vol. 1: *Multiphase Flows*, Chapter 3, Springer, Berlin–Heidelberg (2007), pp. 67–97.
17. V. Laykhovsky, S. Hurwitz, and O. Navon, "Bubble growth in rhyolitic melts: experimental and numerical investigation," *Bull. Volcanol.*, **58**, No. 1, pp. 19–32.
18. V. K. Kedrinskii, M. N. Davydov, A. A. Chernov, and K. Takayama, "Initial stage of the explosive eruption of volcanoes: magma state dynamics in unloading waves," *Dokl. Ross. Akad. Nauk*, **407**, No. 2, 190–193 (2006).